Shear Strength of Assemblies of Frictionless Particles

Bei-Bing Dai[1] and Jun Yang, F.ASCE[2]

Abstract: Whether a granular assembly of frictionless particles has shear strength is a very interesting but not well-understood question. This study addressed this question using discrete element method (DEM) simulations along with an energy-based analysis. It is shown that the use of artificial damping in DEM simulations leads to a frictionless assembly exhibiting normal quasi-static shear behavior, with the overall angle of friction at the critical state being nonzero. However, when this artificial damping is absent, the frictionless assembly cannot achieve a quasi-static state but rather exhibits a stress oscillating state, with all particles in vibration, and the shear strength is expected to be zero. From an energy perspective, it is shown that the artificial damping used in DEM simulations plays the sole role in energy dissipation for the frictionless assembly and that it facilitates the establishment of a quasi-static state from which shear strength is mobilized. Therefore, the nonzero angle of shear resistance reported in the literature for frictionless granular assemblies under quasi-static shear should be regarded as a false rather than a true strength parameter. **DOI: 10.1061/(ASCE)GM.1943-5622.0001005.**

Author keywords: Granular material; Shear strength; Friction angle; Damping; Energy dissipation.

Introduction

Owing to their inherently discrete nature, the mechanical behavior of granular materials is highly complex. In past decades, the linkage between the basic particle attributes and the overall mechanical behavior of granular media have been extensively investigated [e.g., Skinner (1969), Ni et al. (2000), Ng (2004), Cho et al. (2006), Antony and Kruyt (2009), Cavarretta et al. (2010), Abedi and Mirghasemi (2011), Yang and Wei (2012), Yang et al. (2012), Barreto and O'Sullivan (2012), Cole (2015), Yang and Luo (2015), Dai et al. (2015, 2016a), and Yang et al. (2016)]. The influence of interparticle friction is a major concern. Fig. 1 shows the variation of the overall friction angle at the critical state (ϕ_{cs}) with the interparticle friction angle (ϕ_{μ}), obtained from various numerical simulations using the discrete element method (DEM). Due to the use of idealized numerical models, the values for friction angle in the DEM simulation are in general lower than those obtained from laboratory tests on real soil [e.g., Bolton (1986), Santamarina and Cho (2001), Yang and Luo (2015), and Xiao et al. (2016)]. Of particular interest in Fig. 1 is the idealized case where interparticle friction is absent (i.e., $\phi_{\mu} = 0°$). The results of Oger et al. (1998), Maeda et al. (2006), Kruyt and Rothenburg (2006), and Peña et al. (2008) indicated that the overall friction angle ϕ_{cs} is a nonzero value, ranging from 5° to 11°. The simulations of Thornton (2000) and Suiker and Fleck (2004) showed that ϕ_{cs} approximately approaches zero at $\phi_{\mu} = 0°$. The theoretical prediction of Bishop (1954) also suggested that the macroscopic angle of friction should be zero at $\phi_{\mu} = 0°$. The contradictory results in the literature raise a question that is of fundamental interest: does an assembly of frictionless particles have shear strength?

Note that the ideal case of $\phi_{\mu} = 0°$ cannot be achieved in real laboratory experiments but can only be obtained in DEM simulations. In most DEM simulations, in addition to the friction damping generated from the interaction of particles, artificial damping (contact damping or global damping) is usually adopted to dissipate the energy so that computation efficiency is enhanced (Cundall and Strack 1979). In the special case of $\phi_{\mu} = 0°$, no dissipation of frictional energy occurs and artificial damping is thus expected to play a central role in so-called quasi-static shearing. To gain a fundamental understanding of the question, a series of DEM simulations of biaxial shear tests are designed and carried out in this study, with particular attention paid to the role of artificial damping. Analysis is also conducted from the perspective of energy conservation to examine the origin of the shear strength in frictionless assemblies.

Numerical Implementation

The DEM program *PFC2D* was employed to do the numerical simulations of biaxial shear tests. All specimens consisting of frictionless disks are 25×25 mm^2, and they were prepared by the expansion method, so that the potential effect of anisotropy was eliminated. According to the method of statistical analysis adopted by Dai et al. (2015, 2016b), the anisotropy magnitude of contact orientations was determined to be 9×10^{-3}, which indicates an almost isotropic state. The particle size distribution curve is given in Fig. 2. Three groups of biaxial shear tests in which the damping conditions were varied were conducted. The specimens in Group I were sheared in the drained condition, with the damping ratio ranging from 0.01 to 0.7. In the simulation, the quasi-static shear was ensured by introducing a cycling requirement that specified an upper limit for the ratio between the maximum unbalanced force and the average contact force (1‰ in this study). During shear, the ratio between the maximum unbalanced force and the average contact force was monitored, and additional cycling was executed if the ratio value exceeded this specified upper limit. Similar criteria have been used by other researchers in carrying out DEM simulations [e.g., Li (2006), Ng (2006), and Mahmud Sazzad (2014)]. For the specimens in Group II, a quasi-dynamic shear, which refers to monotonic shearing without the control of the unbalanced forces, was executed in the undrained mode with the damping and interparticle friction set to zero. In this

[1]Associate Professor, Research Institute of Geotechnical Engineering and Information Technology, Sun Yat-sen Univ., Guangzhou 510275. China (corresponding author). E-mail: beibing_dai@yahoo.com, daibb@mail.sysu.edu.cn

[2]Associate Professor, Dept. of Civil Engineering, Univ. of Hong Kong, Hong Kong, China. E-mail: junyang@hku.hk

Note. This manuscript was submitted on October 9, 2016; approved on May 24, 2017; published online on September 8, 2017. Discussion period open until February 8, 2018; separate discussions must be submitted for individual papers. This paper is part of the ***International Journal of Geomechanics***, © ASCE, ISSN 1532-3641.

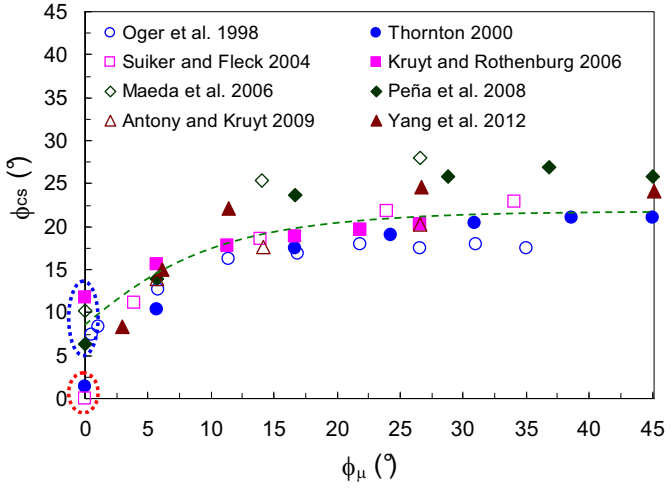

Fig. 1. Relationship between the critical-state friction angle ϕ_{cs} and the interparticle friction angle ϕ_{μ}

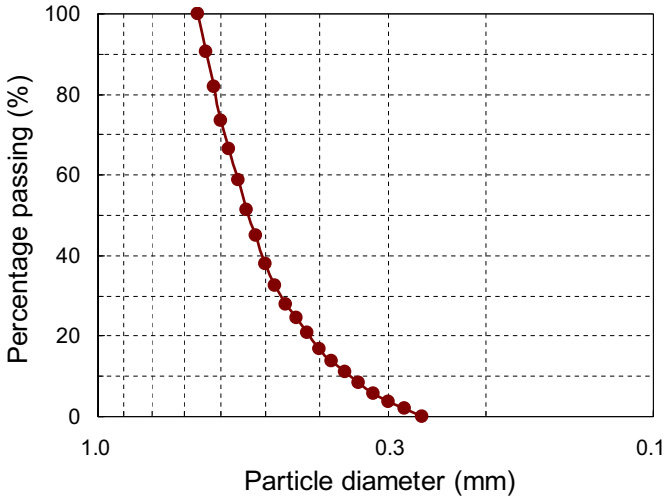

Fig. 2. Particle size distribution curve in present study

execution, the ratio between the maximum unbalanced force and the average contact force was not monitored, and the unbalanced state of the granular system was not adjusted to achieve quasi-static shear through additional cycling. In Group III, a quasi-static shear was tried at zero damping and zero interparticle friction, with the same cycling requirement as used in Group I. Note that the drained shear is not applicable for the cases in Groups II and III, due to the difficulty of controlling constant confining stresses, and undrained shear is thus adopted. The nonzero interparticle friction coefficient is initially used to prepare numerical specimens with a normal packing state. In the subsequent consolidation and shearing processes, the interparticle friction is reset to zero. The loading rate is set at an extremely low level, $\Delta\varepsilon_a = 8.0 \times 10^{-8}$/step. Tables 1 and 2 give the modeling and specimen information.

The damping mechanism introduced in this study is the local damping defined in *PFC2D* and is applied in the equations of motion given by

$$m\ddot{x}_i = \sum F_i - D\left|\sum F_i\right| \mathrm{sgn}(\dot{x}_i) \qquad i = 1, 2 \tag{1}$$

$$I\ddot{\theta} = \sum M - D\left|\sum M\right| \mathrm{sgn}(\dot{\theta}) \tag{2}$$

Table 1. Parameters Used in the Simulations

Model parameter	Value
Particle density [ρ, (g/cm^3)]	2.65
Interparticle sliding and rolling friction (μ_s and μ_r)	0.0
Wall friction (μ_w)	0.0
Normal and tangential stiffness [k_n and k_t (N/m)]	1.0×10^9
Wall stiffness [k_w (N/m)]	1.0×10^9

Table 2. Sample Information

Test group	Test name	Shear mode	p_0 (kPa)	e_0	PN	D	μ_{ini}
Group I	TS-1	Quasi-static	100	0.196	2936	0.01	0.1
	TS-2	Quasi-static	100	0.196	2936	0.1	0.1
	TS-3	Quasi-static	100	0.196	2936	0.3	0.1
	TS-4	Quasi-static	100	0.196	2936	0.7	0.1
Group II	TS-5	Quasi-dynamic	100	0.196	2936	0	0.1
	TS-6	Quasi-dynamic	500	0.195	2936	0	0.1
Group III	TS-7	Quasi-static (trial)	100	0.196	2936	0	0.1

Note: p_0 = initial confining stress; e_0 = initial void ratio; PN = particle number; D = damping ratio; μ_{ini} = friction coefficient before consolidation.

where m and I are the mass and moment of inertia of the particle, $\ddot{x}_i$ and $\dot{x}_i$ are the components of translational acceleration and velocity, $\ddot{\theta}$ and $\dot{\theta}$ are the angular acceleration and velocity, ΣF_i is the components of the resultant out-of-balance force, ΣM is the out-of-balance moment, and D is the damping coefficient. The local damping represents the effect of dashpots connecting the particle with the ground, and it can be thus considered as equivalent to the global damping in Cundall and Strack (1979), in which the damping force and moment are related respectively to the translational and angular velocities through the damping coefficient. At a given instant, it would appear difficult to make an overall estimation of the damping effect based on all the individual damping forces and moments and establish a direct relationship between artificial damping and the global shear strength at a microscopic level, but this does not influence the discussion of the themed issue. The definition of the stresses and strains in this study follows that of Yang and Dai (2011).

The aim of this study is exactly to explore the possible reasons for the contradictory results on whether a granular assembly of particles has a nonzero bulk friction angle if interparticle friction is absent. The assembly of frictionless particles is an ideal case, but it is for this ideal case the controversy arises. The effects of particle shape, loading paths and/or boundary conditions on the bulk behavior of more realistic granular materials (with nonzero interparticle friction), are beyond the scope of this study. In terms of the boundary effect, many researchers have adopted similar 2D numerical models and obtained reasonable results in their simulations (Olivera Bonilla 2004; Li and Yu 2010, 2013; Gu et al. 2013). In particular, the use of frictionless boundary wall and particles in this study will mitigate the boundary effect.

Simulation Results

Shear Behavior with Artificial Damping

Fig. 3 shows the shear responses of the specimens in Group I (TS-1 to TS-4). The level of shear strain in this study is comparable to that found in Thornton (2000). Although these specimens are sheared under different damping conditions, they demonstrate similar shear

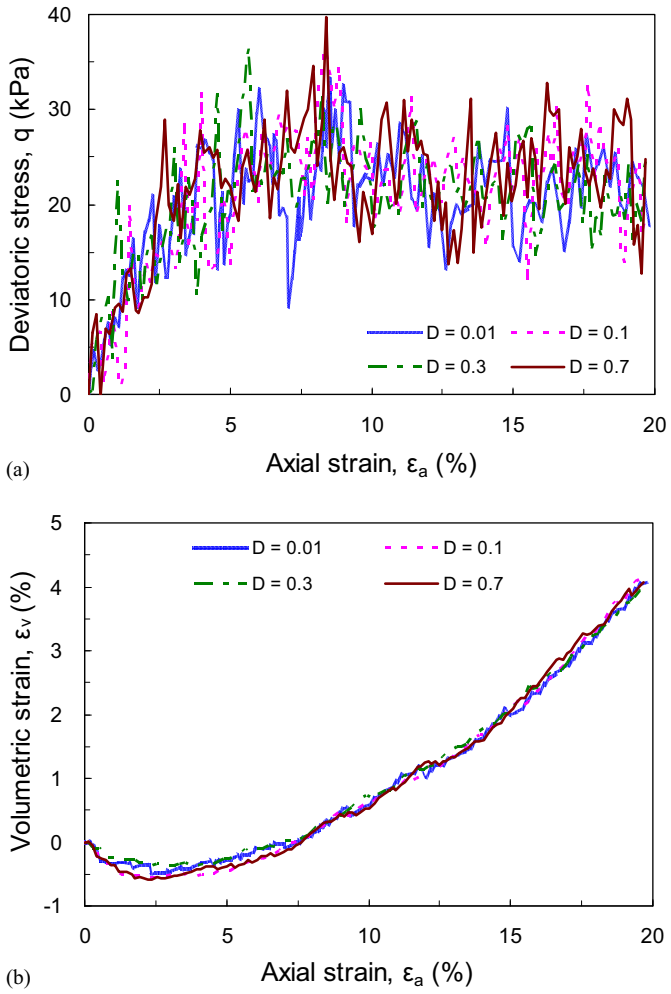

Fig. 3. Quasi-static shear behaviors of specimens with the introduction of damping ($p_0 = 100$ kPa, $\phi_\mu = 0°$ and D $\neq$ 0): (a) q versus ε_a; (b) ε_v versus ε_a

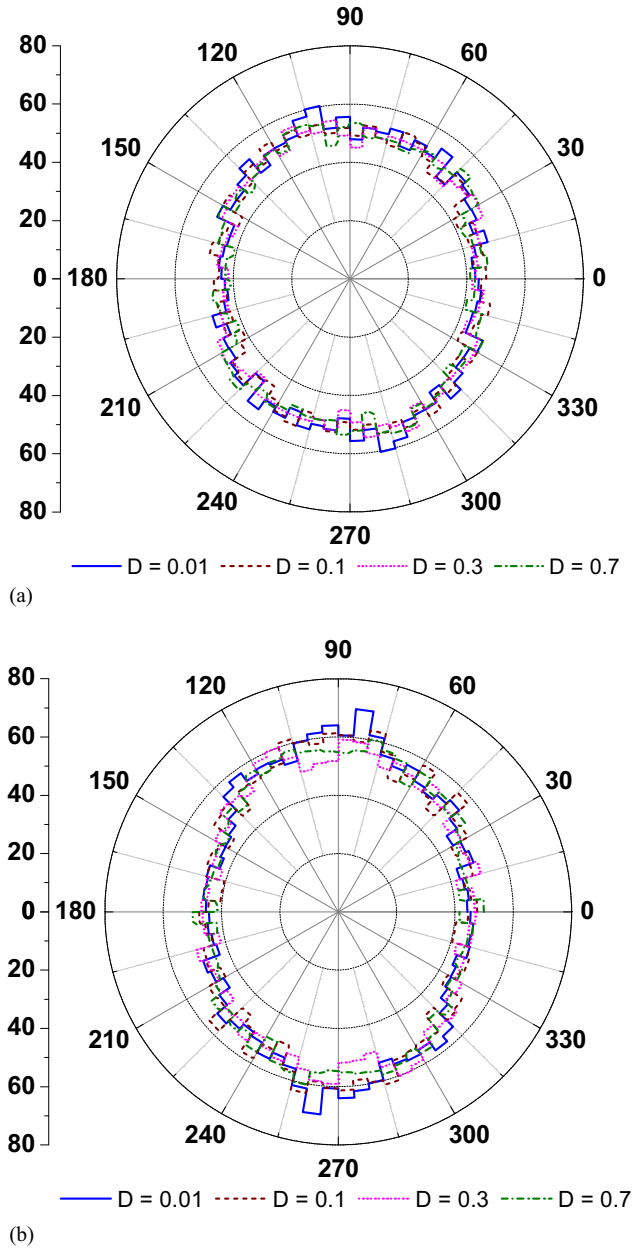

Fig. 4. Angular distribution of contact normal forces (N) measured by the vertical axis ($\phi_\mu = 0°$ and D $\neq$ 0): (a) $\varepsilon_a = 2\%$; (b) $\varepsilon_a = 15\%$

behaviors (Fig. 3). At the grain scale, the angular distributions of normal contact forces at different strain levels are also almost the same (Fig. 4). These results suggest that the influence of varying damping is insignificant. Li (2006) also observed insignificant influence of varying damping coefficients on the overall behavior of granular assemblies under quasi-static shear. However, it is worth noting that the deviatoric stress q exhibits distinct fluctuations during shear under different damping conditions. This may suggest that the frictionless granular system is metastable, and a tiny step of shear loading can lead to a considerable disturbance and subsequently intense particle motions that need to be stabilized by the artificial damping mechanism for a quasi-static shear. This is because in the zero interparticle friction condition, intense and rapid particle rearrangements may occur. The loading rate $\Delta\varepsilon_a = 8.0 \times 10^{-8}$/step is considered to be reasonably low compared to that of published studies on frictionless assemblies (e.g. Peña et al. 2008; Thornton 2000).

In Fig. 3(b), the evolution of volumetric strain does not reach a plateau stage at large shear strains, indicating that the critical state is not yet achieved. To determine the critical-state friction angle ϕ_{cs}, the stress-dilatancy data is fitted by the Rowe's stress-dilatancy equation (Wood 1990; Dai et al. 2016b), in which the soil friction angle ϕ_f is taken to be the critical-state friction angle ϕ_{cs}. The use of Rowe's stress-dilatancy relationship to derive the friction angle in a critical state has been adopted by a number of researchers, for example, Zhang and Salgado (2010) and Simoni and Houlsby (2006). A similar approach has also been adopted by Bolton (1986) in his analysis of experimental data sets from published literature on sands. The advantage of this approach is that it minimizes the influence of uncertainty associated with the determination of the critical state at large strains. It should be pointed out that the best fit analysis with the Rowe's stress-dilatancy relationship was done with respect to the whole shearing process rather than a particular shearing state. As shown in Fig. 5, the value of ϕ_{cs} is not zero but takes a value of about 5°, which is quite close to the values reported in the literature for frictionless assemblies (Fig. 1).

Shear Behavior without Artificial Damping

Fig. 6 shows the overall responses of the two specimens TS-5 and TS-6 in Group II, which are subjected to a quasi-dynamic shear

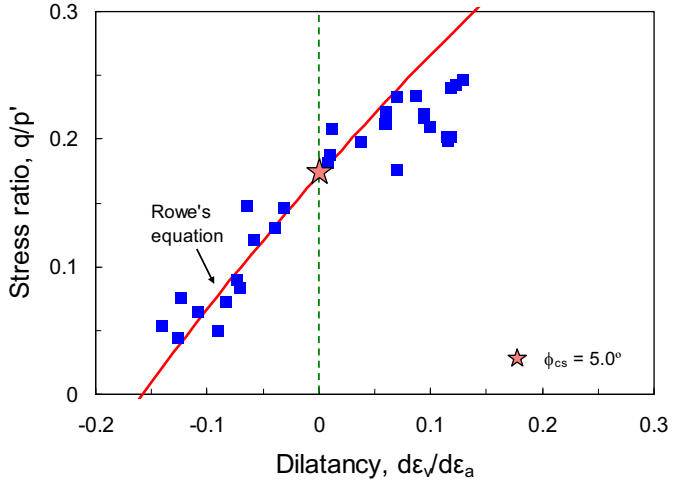

Fig. 5. Stress-dilatancy relationship ($\phi_\mu = 0°$ and $D \neq 0$): q/p' vs. $d\varepsilon_v/d\varepsilon_a$

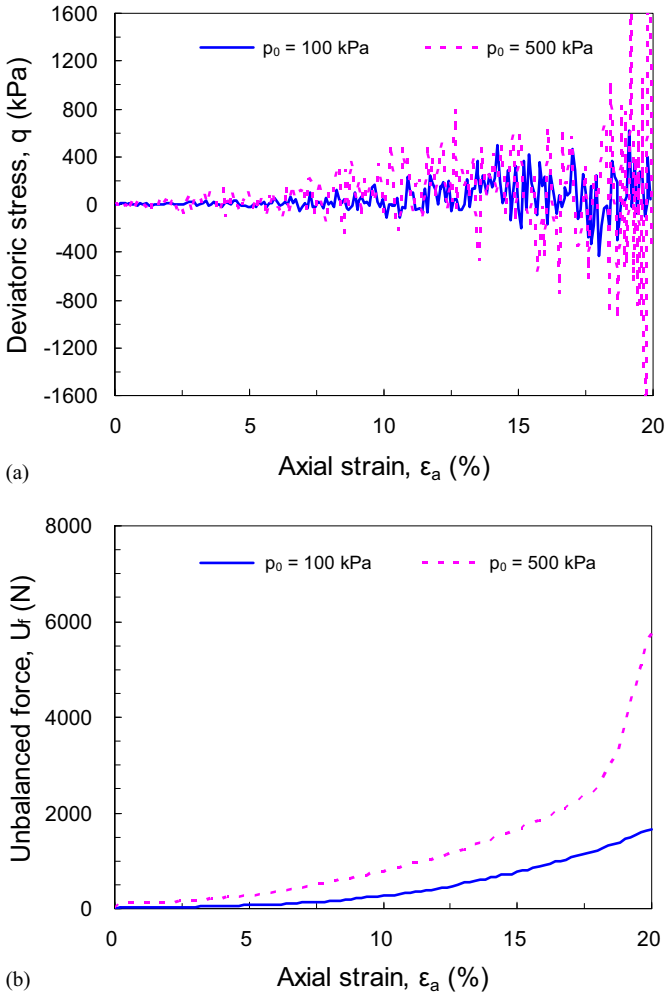

Fig. 6. Quasi-dynamic shear behaviors of specimens without the introduction of damping ($\phi_\mu = 0°$ and $D = 0$) (TS-5 and TS-6): (a) q versus ε_a; (b) U_f versus ε_a

without setting a cycling requirement with respect to the unbalanced force. The deviatoric stress q in Fig. 6(a) is nearly zero when the axial strain ε_a is less than 2.5%. Beyond this strain level, it starts to fluctuate approximately about a neutral zero value, and the fluctuations are persistently exacerbated as shearing goes on. Fig. 6(b) shows that the average unbalanced force U_f is at an almost constant low level during the initial shearing, which is then followed by a marked increase. As shown in Fig. 7(a), the coordination numbers of these two cases, which refer to the average contact numbers per particle, are both around 4 at the initial state and decrease rapidly upon shearing; then they tend to maintain at a low level (below 3) in the subsequent shearing, with the minimum coordination number being around 2.5. Fig. 7(b) shows a continuous increase of kinetic energy for these two specimens. The simulations indicate that persistent shearing without artificial damping makes an initially static granular system transit toward an oscillating system in which the individual particles are all in a vibration mode.

For comparison, in Group III a quasi-static shear without artificial damping is tried on specimen TS-7 with the introduction of the same cycling requirement as is used in Group I. As can be seen in Fig. 8, where the variation of unbalanced force is plotted against the cycling step number after one loading step, no quasi-static shear can be executed for this specimen. The average unbalanced force U_f keeps increasing and undergoes an obvious leap at step number 2.4×10^8, signifying that the instability of the specimen TS-7 is aggravated and no convergence can be achieved for this trial step of loading.

The specifically designed DEM simulations show that only the specimens in Group I can attain a quasi-static shear response from which nonzero critical-state shear strength can be derived. This lends support to the hypothesis that the artificial damping mechanism functions to dissipate energy and thus assists the establishment of a stable particulate system that is capable of sustaining a quasi-static shear. As there is no artificial damping mechanism in the other two groups of numerical simulations, no energy dissipation can take place, and consequently, these granular assemblies are transformed into an oscillating system with all particles in a vibration mode.

Analysis from an Energy Perspective

The simulations indicate that artificial damping plays an important role in the energy dissipation of a granular system. It is thus of interest to examine energy dissipation in DEM simulations in detail. For a triaxial or biaxial compression test, the energy-work equation can be formulated in a general form as (Dai 2010):

$$q d\varepsilon_q + p' d\varepsilon_v = \sum dE_{friction} + \sum dE_{strain} + \sum dE_{kinetic} + \sum dE_{damping} \quad (3)$$

in which q and p' are the deviatoric and mean effective stresses, $d\varepsilon_q$ and $d\varepsilon_v$ are the deviatoric and volumetric strain increments, $dE_{friction}$ is the incremental thermal energy dissipated through particle sliding and rolling, dE_{strain} is the incremental potential energy relating to the elastic deformation of the particles themselves, $dE_{damping}$ is the energy loss induced by damping in the loading step, and $dE_{kinetic}$ is the incremental kinetic energy of particles, which depends on the particle motions, including both translation and rotation. The symbol Σ in Eq. (3) refers to summation over contacts or particles. It is postulated in Eq. (3) that no breakage and plastic deformation occurs in the particles. Generally, each loading step in a DEM simulation involves a process of transforming the input work into the thermal energy dissipated through friction, potential (strain) energy stored at contacts, kinetic energy relating to particle motions, and the energy consumed by damping. Eq. (3) also indicates that two important energy dissipation means exist: friction

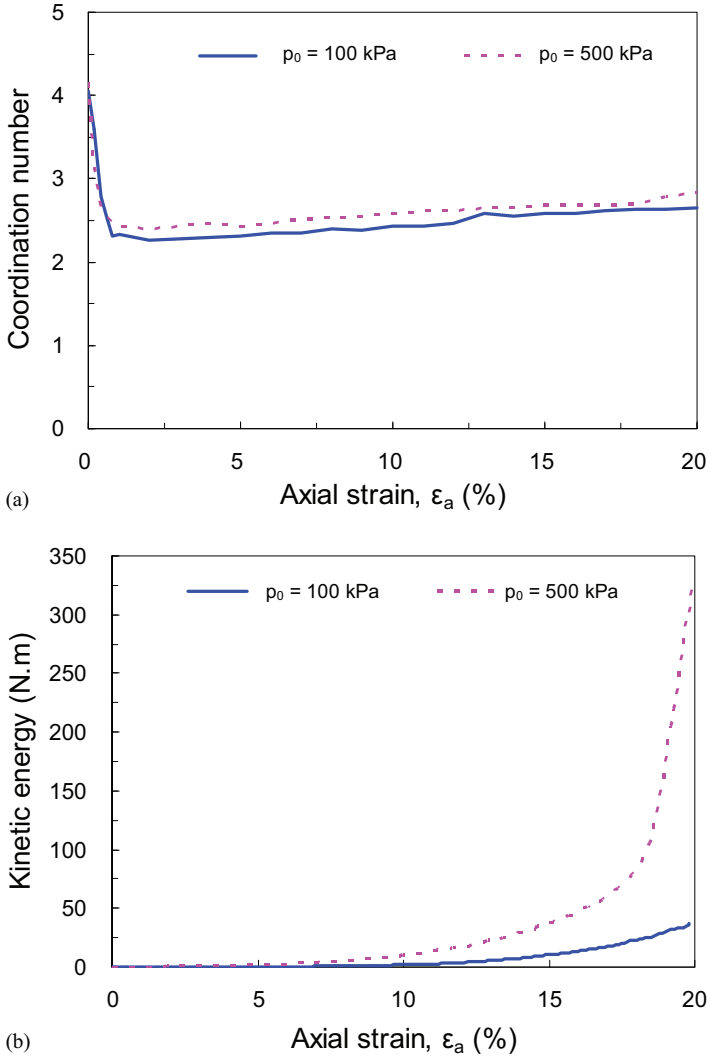

Fig. 7. Evolution of (a) coordination numbers and (b) the kinetic energy of specimens without the introduction of damping ($\phi_\mu = 0°$ and D = 0) (TS-5 and TS-6)

and damping. As far as the special case ($\phi_\mu = 0°$) is concerned, the frictional dissipation is zero, so Eq. (3) is modified to:

$$qd\varepsilon_q + p'd\varepsilon_v = \sum dE_{strain} + \sum dE_{kinetic} + \sum dE_{damping} \quad (4)$$

Fig. 9 depicts the energy responses of the specimens in Group I. The first two plots show that the input work and the damping consumed energy evolve in almost the same manner during shear, suggesting that most input work is consumed by the damping mechanism. The kinetic energy and strain energy are calculated by executing integrated commands built into the software. The damping consumption is worked out by deducting the kinetic energy of the particles and strain energy stored at contacts from the total input work. Note that aside from some occasional spikes, kinetic energy, as shown in Fig. 9(c), is at a low level (below $\sim 4.0 \times 10^{-5}$ N·m) and its increment $\Sigma dE_{kinetic}$ in each loading step can be neglected for a quasi-static shear. As shown in Fig. 9(d), the strain energy for large strains also fluctuates at a very small level ($\sim$0.004 N·m) compared with the damping consumed energy, implying that the incremental strain energy ΣdE_{strain} approximately approaches zero for large strains as well. This observation is in agreement with the DEM simulation result of Kruyt and Rothenburg (2006) that the strain energy tends to be at a constant level for large strains. Hence the energy work equation at the critical state can be further expressed as:

$$qd\varepsilon_q = \sum dE_{damping} \quad (5)$$

It then follows that the input work is entirely dissipated by damping at the critical state and the shear strength depends solely on the energy dissipation through damping. Taking the specimen TS-3 as an example, Fig. 10(a) shows that the evolution of input work against shear strain almost overlaps with that of the damping consumed energy. At large shear strains, the energy loss induced by damping accounts for nearly 100% of the total input work [Fig. 10(b)].

Concluding Remarks

For the special case $\phi_\mu = 0°$, artificial damping plays the sole role in energy dissipation in DEM simulations, contributing to the achievement of a quasi-static shear. It can therefore be thought that energy dissipation through damping helps build up a stable energy system at a quasi-static state, based on which the shear strength is

mobilized. Without the effect of damping, a stable energy-work system cannot be established in a quasi-static state and shear strength at the critical state should be zero according to Eq. (5).

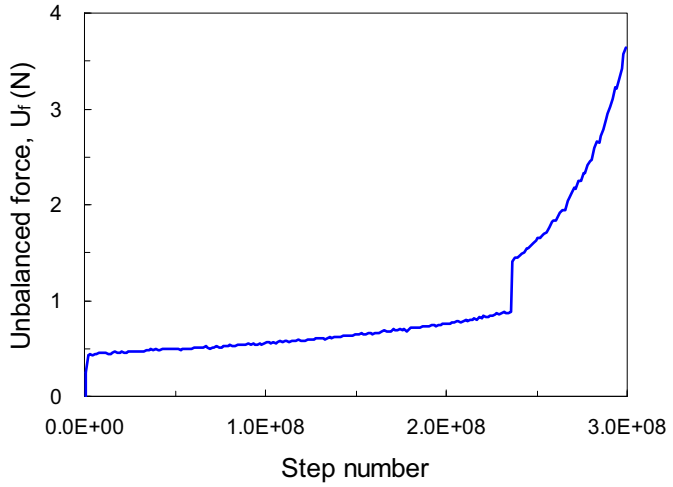

Fig. 8. Evolution of unbalanced forces for the specimen in a trial quasi-static shear ($\phi_\mu = 0°$ and D = 0) (TS-7)

This view is, to some extent, validated by the DEM simulations of specimens in Groups II and III. Note that the deviatoric stress, as shown in Fig. 6(a), is nearly zero under low-input work in the initial shearing stage and no shearing can be performed on the specimen TS-7. These observations suggest that an idealized frictionless granular medium is unable to sustain any shear load, and accordingly that the shear strength should be zero. This deduction is congruous to the DEM simulation results of Thornton (2000) and Suiker and Fleck (2004), which indicated that the critical-state friction angle ϕ_{cs} is close to zero at $\phi_\mu = 0°$.

According to the DEM simulations in this study, the nonzero critical-state friction angle reported in the literature for assemblies of frictionless particles is ascribed to the energy dissipation through damping. It is thought that the artificial damping mechanism, including the global damping in Cundall and Strack (1979) and local damping in *PFC2D*, does not represent the real damping mechanisms associated with the interactions at particle contacts in the form of sliding and rolling and plastic deformation. Although contact damping, which is also referred to as viscous contact damping, has physical significance and is connected with viscous contact behavior or inelastic collisions between particles, it is usually artificially utilized by researchers as an auxiliary measure of computation to achieve rapid convergence to the equilibrium configuration, and its use does not reflect or relate to any real physical situation.

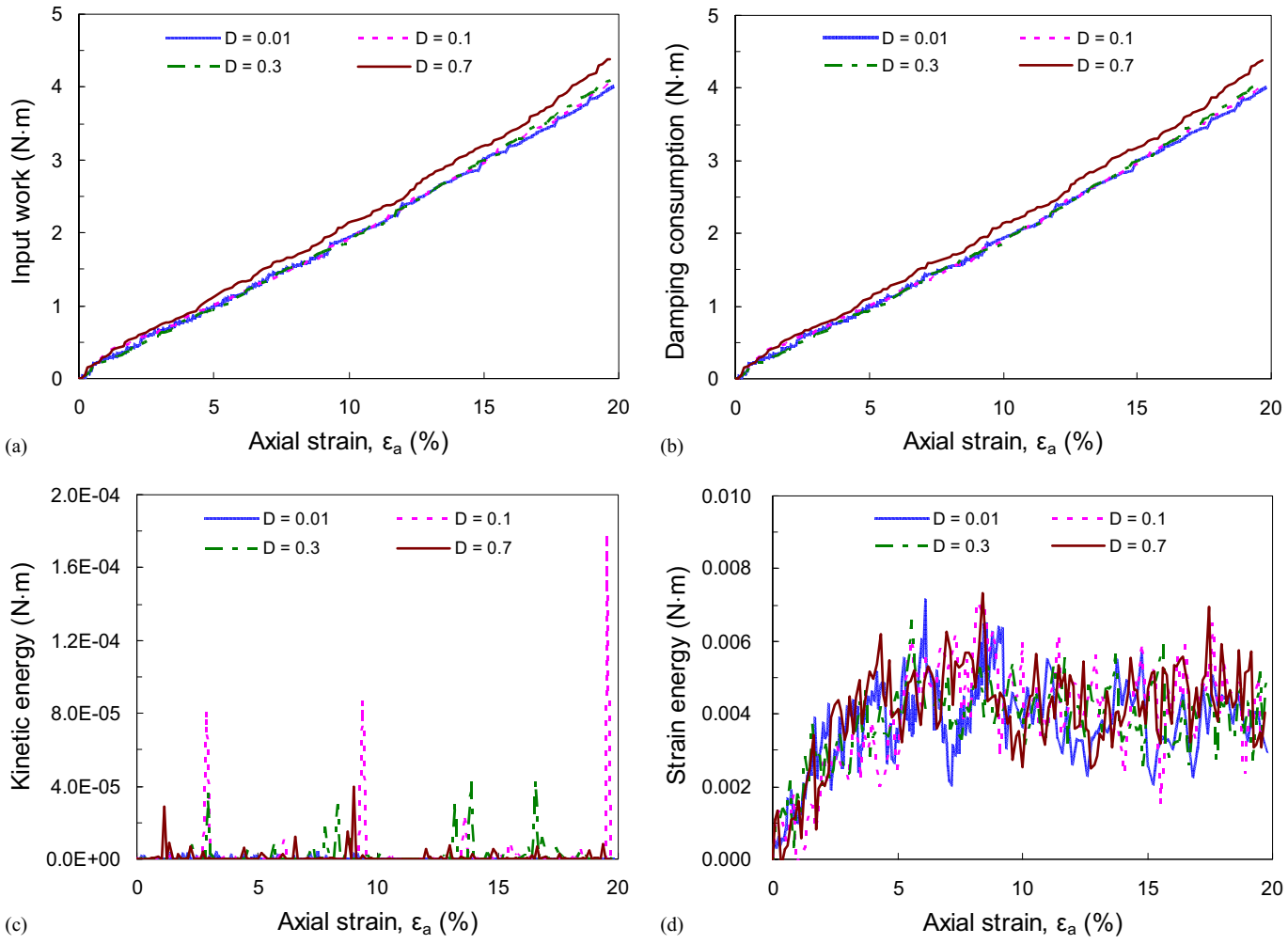

Fig. 9. Energy responses of specimens with the introduction of damping ($\phi_\mu = 0°$ and $D \neq 0$): (a) input work; (b) damping consumption; (c) kinetic energy; (d) strain energy

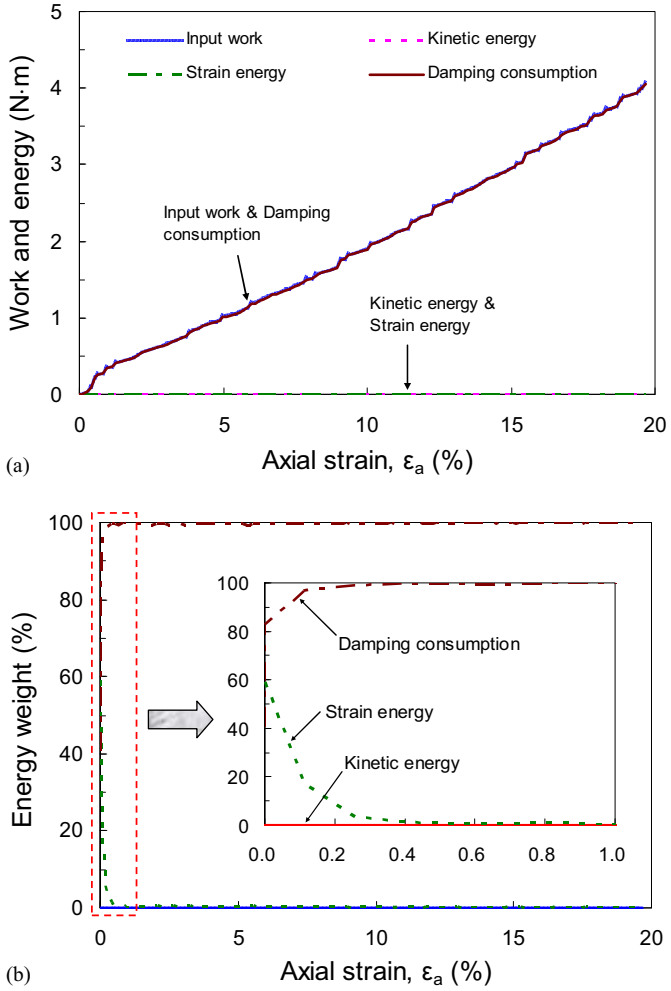

Fig. 10. (a) Energy responses and (b) energy weights for the specimen TS-3

For instance, Peña et al. (2008, p. 146) "introduce a viscous force, which is necessary to maintain the numerical stability of the method and to obtain a quick convergence to the equilibrium configuration." Hence the shear strength obtained from DEM simulations in the absence of interparticle friction, in which artificial damping is used or a damping mechanism is artificially used, should not be treated as the true strength.

Acknowledgments

The authors extend their sincere gratitude to the financial support provided by the National Natural Science Foundation of China (51209237, 51428901) and the Fundamental Research Funds for the Central Universities (13lgpy05).

Notation

The following symbols are used in this paper:

q = deviatoric stress;
p' = mean effective stress;
ε_v = volumetric strain;
ε_q = deviatoric strain;
ε_a = axial strain;
ϕ_μ = inter-particle friction angle;
ϕ_{cs} = critical-state friction angle;
D = damping ratio;
U_f = unbalanced force;
μ (μ_s) = inter-particle (sliding) friction coefficient;
μ_r = inter-particle rolling friction coefficient;
μ_w = wall friction coefficient;
k_w = wall stiffness;
k_n = normal stiffness;
k_t = tangential stiffness;
E_{strain} = strain energy stored at contacts;
$E_{kinetic}$ = kinetic energy of particles;
$E_{friction}$ = frictional dissipation energy; and
$E_{damping}$ = energy loss induced by damping.

References

Abedi, S., and Mirghasemi, A. A. (2011). "Particle shape consideration in numerical simulation of assemblies of irregularly shaped particles." *Particuology*, 9(4), 387–397.
Antony, S. J., and Kruyt, N. P. (2009). "Role of interparticle friction and particle-scale elasticity in the shear-strength mechanism of three-dimensional granular media." *Phys. Rev. E*, 79(3), 031308.
Barreto, D., and O'Sullivan, C. (2012). "The influence of inter-particle friction and the intermediate stress ratio on soil response under generalised stress conditions." *Granular Matter*, 14(4), 505–521.
Bishop, A. W. (1954). "Correspondence on shear characteristics of a saturated silt, measured in triaxial compression." *Géotechnique*, 4(1), 43–45.
Bolton, M. D. (1986). "The strength and dilatancy of sands." *Géotechnique*, 36(1), 65–78.
Cavarretta, I., Coop, M., and O'Sullivan, C. (2010). "The influence of particle characteristics on the behaviour of coarse grained soils." *Géotechnique*, 60(6), 413–423.
Cho, G., Dodds, J., and Santamarina, J. C. (2006). "Particle shape effects on packing density, stiffness and strength: natural and crushed sands." *J. Geotech. Geoenviron. Eng.*, 10.1061/(ASCE)1090-0241(2006)132:5(591), 591–602.
Cole, D. M. (2015). "Laboratory observations of frictional sliding of individual contacts in geologic materials." *Granular Matter*, 17(1), 95–110.
Cundall, P. A., and Strack, O. D. L. (1979). "A discrete numerical model for granular assemblies." *Géotechnique*, 29(1), 47–65.
Dai, B. B. (2010). "Micromechanical investigation of the behavior of granular materials." Ph.D. dissertation, Dept. of Civil Engineering, Univ. of Hong Kong, Hong Kong.
Dai, B. B., Yang, J., and Luo, X. D. (2015). "A numerical analysis of the shear behavior of granular soil with fines." *Particuology*, 21, 160–172.
Dai, B. B., Yang, J., and Zhou, C. Y. (2016a). "Observed effects of interparticle friction and particle size on shear behavior of granular materials." *Int. J. Geomech.*, 10.1061/(ASCE)GM.1943-5622.0000520, 04015011.
Dai, B. B., Yang, J., Zhou, C. Y., and Luo, X. D. (2016b). "DEM investigation on the effect of sample preparation on the shear behavior of granular soil." *Particuology*, 25, 111–121.
Gu, X., Yang, J., and Huang, M. (2013). "DEM simulation of the small strain stiffness of granular soils: effect of stress ratio." *Granular Matter*, 15(3), 287–298.
Kruyt, N. P. and Rothenburg, L. (2006). "Shear strength, dilatancy, energy and dissipation in quasi-static deformation of granular materials." *J. Stat. Mech.: Theory Exp.*, P07021.
Li, X. (2006). "Micro-scale investigation on the quasi-static behavior of granular material." Ph.D. dissertation, Department of Civil Engineering, The Hong Kong Univ. of Science and Technology, Hong Kong.
Li, X. and Yu, H.-S. (2010). "Numerical investigation of granular material behaviour under rotational shear." *Géotechnique*, 60(5), 381–394.
Li, X. and Yu, H.-S. (2013). "On the stress-force-fabric relationship for granular materials." *Int. J. Solids Struct.*, 50(9), 1285–1302.
Maeda, K., Hirabayashi, H., and Ohmura, A. (2006). "Micromechanical influence of grain properties on deformation-failure behavior of granular media by DEM." *Proc., Int. Symp. on Geomech. and Geotechnics of*

Particulate Media, M. Hyodo, H. Murata, and Y. Nakat, eds., Taylor & Francis, 173–180.
Mahmud Sazzad, M. (2014). "Micro-scale behavior of granular materials during cyclic loading." *Particuology*, 16, 132–141.
Ng, T.-T. (2004). "Shear strength of assemblies of ellipsoidal particles." *Géotechnique*, 54(10), 659–669.
Ng, T.-T. (2006). "Input parameters of discrete element methods." *J. Eng. Mech.*, 10.1061/(ASCE)0733-9399(2006)132:7(723), 723–729.
Ni, Q., Powrie, W., Zhang, X., and Harkness, R. (2000). "Effect of particle properties on soil behaviour: 3-D numerical modelling of shear box tests." *Geotechnical Special Publication*, 96, 58–70.
Oger, L., Savage, S. B., Corriveau, D., and Sayed, M. (1998). "Yield and deformation of an assembly of disks subjected to a deviatoric stress loading." *Mech. Mater.*, 27(4), 189–210.
Olivera Bonilla, R. R. (2004). "Numerical simulation of undrained granular media." Ph.D. dissertation, Dept. of Civil Engineering, Univ. of Waterloo, Waterloo, ON, Canada.
Peña, A. A., Lizcano, A., Alonso-Marroquin, F., and Herrmann, H. J. (2008). "Biaxial test simulations using a packing of polygonal particles." *Int. J. Numer. Anal. Meth. Geomech.*, 32(2), 143–160.
PFC2D [Computer software]. Itasca Consulting Group, Inc., Minneapolis.
Santamarina, J. C. and Cho, G. C. (2001). "Determination of critical state parameters in sandy soils-simple procedure." *Geotech. Test. J.*, 24(2), 185–192.
Simoni, A. and Houlsby, G. T. (2006). "The direct shear strength and dilatancy of sand-gravel mixtures." *Geotech. Geol. Eng.*, 24(3), 523–549.
Skinner, A. E. (1969). "A note on the influence of interparticle friction on the shear strength of a random assembly of spherical particles." *Géotechnique*, 19(1), 150–157.
Suiker, A. S. J. and Fleck, N. A. (2004). "Frictional collapse of granular media." *J. Appl. Mech*, 71(3), 350–358.
Thornton, C. (2000). "Numerical simulations of deviatoric shear deformation of granular media." *Géotechnique*, 47(2), 319–329.
Wood, D. M. (1990). *Soil behaviour and critical state soil mechanics*, Cambridge University Press, Cambridge, U.K.
Xiao, Y., Liu, H. L., Ding, X. M., Chen, Y. M., Jiang, J. S., and Zhang, W. G. (2016). "Influence of particle breakage on critical state line of rockfill material." *Int. J. Geomech.*, 10.1061/(ASCE)GM.1943-5622.0000538, 04015031.
Yang, J., and Dai, B. B. (2011). "Is the quasi-steady state a real behaviour? A micromechanical perspective." *Géotechnique*, 61(2), 175–184.
Yang, J., and Luo, X. D. (2015). "Exploring the relationship between critical state and particle shape for granular materials." *J. Mech. Phys. Solids*, 84, 196–213.
Yang, Y., Wang, J. F., and Cheng, Y. M. (2016). "Quantified evaluation of particle shape effects from micro-to-macro scales for non-convex grains." *Particuology*, 25, 23–35.
Yang, J., and Wei, L. M. (2012). "Collapse of loose sand with the addition of fines: the role of particle shape." *Géotechnique*, 62(12), 1111–1125.
Yang, Z. X., Yang, J., and Wang, L. Z. (2012). "On the influence of interparticle friction and dilatancy in granular materials: A numerical analysis." *Granular Matter*, 14(3), 433–447.
Zhang, J., and Salgado, R. (2010). "Stress-dilatancy relation for Mohr-Coulomb soil following a non-associated flow rule." *Géotechnique*, 60(3), 223–226.